MAGNETOHYDRODYNAMIC FLOW AND HEAT TRANSFER OVER A MOVING CYLINDER IN A NANOFLUID UNDER CONVECTIVE BOUNDARY CONDITIONS AND HEAT GENERATION

by

Mohamed S. ABDEL-WAHED[a*] and Essam M. EL-SAID[b]

[a] Basic Sciences Department, Faculty of Engineering at Benha, Benha University, Cairo, Egypt
[b] Basic Sciences Department, El Gazeera High Institute for Engineering and Technology, Cairo, Egypt

Original scientific paper
https://doi.org/10.2298/TSCI170911279A

In this paper, the effect of convective boundary conditions, heat generation, Brownian motion, and thermophoresis on heat transfer characteristics of a moving cylinder embedded into cooling medium consists of water with nanoparticles are studied. The governing boundary-layer equations transformed to ODE using similarity transformation method and then solved analytically using optimal homotopy asymptotic method for the general case. The velocity, temperature, and concentration profiles within the boundary-layer plotted and discussed in details for various values of the different parameters. Moreover, the effect of boundary-layer behavior on the surface shear stress, rate of heat and mass transfer investigated.

Key words: *nanofluids, moving cylinder, convective boundary conditions, heat generation, optimal homotopy asymptotic method*

Introduction

The boundary-layer flow caused by a moving surface or cylinder has drawn the attention of many researchers due to its important applications in the industry process such as paper production, wires extrusion *etc.* also the study of boundary-layer behavior over a moving cylinder during the process of cooling is a mathematical simulation to the process of heat treatment of metals. Ali Chamkha [1] studied the MHD boundary-layer over a moving cylinder under the influence of heat generation and chemical reaction. Swati [2] analyzed the boundary-layer over a stretching cylinder in porous medium. Elbashbeshy *et al*. [3] investigated the effect of heat source and suction/injection on the heat transfer characteristics of MHD boundary-layer over a horizontal stretching cylinder. Rekha and Naseen [4] studied the behavior of the boundary-layer over a stretching cylinder under variable thermal conductivity.

Because the main property of the cooling fluid is the heat absorption due to its high thermal conductivity, so the nanofluids became the appropriate for this process. Choi *et al*. [5] suggested these fluids to improve the thermal conductivity of the water by adding very fine particles that's in nanosized. From this date, many researchers focus their efforts to investigate the influence of these types of fluids on the heat transfer characteristics. Azizah *et al*. [6] studied the time-dependent motion of a shrinking sheet within nanofluid. Aminreza *et al.* [7] studied the effect of partial slip boundary condition on the flow of nanofluids over

* Corresponding author, e-mail: eng_moh_sayed@live.com, essamscience@gmail.com

stretching sheet. Hamad [8] analyzed analytically the natural convection MHD flow of nanofluids over a stretching sheet. Alsaedi *et al.* [9] investigated the influence of heat generation on a stagnation point nanofluid boundary-layer under convective boundary conditions. Elbashbeshy *et al.* [10] presented an exact solution for the MHD nanofluid boundary-layer over a moving surface under the influence of suction/injection. Elbashbeshy *et al.* [11] studied the behavior of the boundary-layer over a moving surface with variable thickness under the effect of thermal radiation. Abdel-wahed *et al.* [12] investigated the effect of the thermophoresis force and the Brownian motion of the nanofluids on the boundary-layer over a moving surface with variable thickness. Abdel-wahed [13] studied the effect of the micro-rotation element on the nanofluid boundary-layer over flat surface. Hayat *et al.* [14] investigated the influence of convective boundary conditions on MHD flow of nanofluid over a stretching sheet. Nazar *et al.* [15] studied the mixed convection boundary-layer of nanofluid over horizontal cylinder. Anbuchezhian [16] investigated the effect of the thermophoresis force and the Brownian motion of nanofluid on a boundary-layer subjected to thermal radiation. Ali *et al* [17] studied the transient natural convection flow of a nanofluid over vertical cylinder. Elbashbeshy *et al.* [18] investigated the effect of heat treatment process with nanofluids as new coolants on the mechanical properties of a moving cylinder. Elbashbeshy *et al.* [19] extended their previous work to study the effect of the thermal radiation and heat generation on the mechanical properties of a moving cylinder during the cooling process. Abdel-wahed *et al.* [20, 21] studied the effect of joule heating and hall current on the MHD nanofluid flow over a rotating disk in the presence of non-linear thermal radiation. Nadeem *et al.* [22] studied the 3-D boundary-layer of cassone nanofluid over a stretching sheet with convective boundary conditions.

The objective of the present work is to study the effect of convective boundary conditions, heat generation and hydromagnetic flow on the boundary-layer behavior and the impact of these forces on the surface shear stress, heat and mass transfer over a moving cylinder in a nanofluid.

Formulation of the problem

Consider a steady, incompressible, laminar, 2-D flow of a viscous electrically conduction nanofluid over a continuous moving cylinder in the presence of heat generation, Q_0. Assume the induced magnetic field produced by the motion of an electrically conducting fluid is negligible, this assumption is valid for small magnetic Reynolds number. Further, since there is no external electric field, the electric field due to polarization of charges is negligible. Moreover, we considered the bottom surface of the cylinder is heated by convection from a hot fluid at temperature, T_f, and concentration, C_f, which provide a heat transfer coefficient, h, and mass transfer coefficient, k_m, respectively. Moreover, assume that both the fluid phase and nanoparticles are in thermal equilibrium state and no slip occurs between them. The physical model of the problem shown in fig. 1

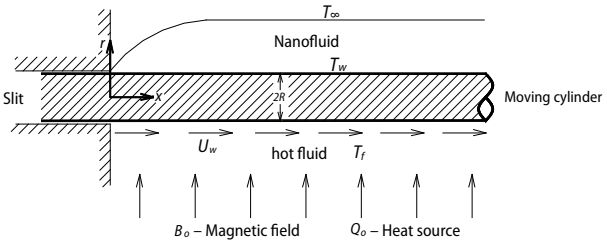

Figure 1. Physical model and co-ordinate system

The governing boundary-layer equations for the steady 2-D laminar nanofluid flows over a moving cylinder can be written as [14, 19]:

$$\frac{\partial}{\partial x}(r\,u)+\frac{\partial}{\partial r}(r\,v)=0 \tag{1}$$

$$u\frac{\partial u}{\partial x}+v\frac{\partial u}{\partial r}=\left(\frac{\upsilon}{r}\right)\frac{\partial}{\partial r}\left(r\frac{\partial u}{\partial r}\right)-\left(\frac{\sigma\beta_0^2}{\rho^*}\right)u \tag{2}$$

$$u\frac{\partial T}{\partial x}+v\frac{\partial T}{\partial r}=\left(\frac{\alpha}{r}\right)\frac{\partial}{\partial r}\left(r\frac{\partial T}{\partial r}\right)+\tau\left[D_B\frac{\partial C}{\partial r}\frac{\partial T}{\partial r}+\frac{D_T}{T_\infty}\left(\frac{\partial T}{\partial r}\right)^2\right]+\frac{Q_0}{\rho^* Cp}(T-T_\infty) \tag{3}$$

$$u\frac{\partial C}{\partial x}+v\frac{\partial C}{\partial r}=\left(\frac{D_B}{r}\right)\frac{\partial}{\partial r}\left(r\frac{\partial C}{\partial r}\right)+\frac{D_T}{T_\infty}\frac{\partial}{r\,\partial r}\left(r\frac{\partial T}{\partial r}\right) \tag{4}$$

with boundary conditions:

$$\begin{gathered}u=U_w,\quad v=0,\quad -k\frac{\partial T}{\partial y}=h\,(T_f-T),\quad -D_m\frac{\partial C}{\partial y}=k_m(C_f-C),\quad \text{at}\quad r=R\\ u=0,\quad v=0,\quad T=T_\infty\quad as\quad r\to\infty\end{gathered} \tag{5}$$

where u and v are velocity components in the x- and r-directions, respectively, υ – the kinematic viscosity, ρ^* – the density of the base fluid, σ – the electrical conductivity, α – the thermal diffusion, D_B – the Brownian diffusion coefficient, D_T – the thermophoretic diffusion coefficient, D_m – the molecular diffusivity, k_m – the surface mass transfer coefficient, h – the conective heat transfer coefficient, and τ – the ratio between the effective heat capacity of the nanoparticle and heat capacity of the fliud.

The velocity of the cylinder is assumed in the form:

$$U_w(x)=a\,x \tag{6}$$

where a is constant.

Similarity analysis and numerical procedure

Looking for similarity solution of eqs. (1)-(4) with the boundary conditions (5) using the following definitions:

$$\eta=\frac{r^2-R^2}{2R}\sqrt{\frac{a}{\upsilon}},\quad \psi=\sqrt{a\upsilon}\,x\,R\,f(\eta),\quad \theta(\eta)=\frac{T-T_\infty}{T_f-T_\infty},\quad \phi(\eta)=\frac{C-C_\infty}{Cf-C_\infty} \tag{7}$$

where η is the similarity variable, $\theta(\eta)$ – the dimensionless temperature, $\phi(\eta)$ – the dimensionless concentration, and ψ – the stream function which is defined as $u=\partial\psi/(r\,\partial r)$ and $v=-\partial\psi/(r\,\partial x)$ which satisfies eq. (1), substituting eq. (7) into eqs. (2)-(4), we obtain the following ordinary differential equations:

$$(1+2\eta\rho)f'''+2\rho f''+ff''-f'^2-M\,f'=0 \tag{8}$$

$$(1+2\eta\rho)\left[\theta''+\Pr Nb\,\theta'\phi'+\Pr Nt\,\theta'^2\right]+(2\rho)\theta'+\Pr f\theta'+\Pr\delta\theta=0 \tag{9}$$

$$(1+2\eta\rho)\left[\phi''+\left(\frac{Nt}{Nb}\right)\theta''\right]+2\rho\phi'+\rho\left(\frac{Nt}{Nb}\right)\theta'+\mathrm{Le}\,f\phi'=0 \tag{10}$$

with boundary conditions:

$$f(0)=0,\quad f'(0)=1,\quad \theta'(0)=-\gamma_1\ \left[1-\theta(0)\right],\quad \phi'(0)=-\gamma_2\ \left[1-\phi(0)\right] \text{ and}$$
$$f'(\infty)=0,\quad \theta(\infty)=0,\quad \phi(\infty)=0 \tag{11}$$

here primes denote differentiation with respect to (η) where:

$$\mathrm{Pr}=\frac{\upsilon}{\alpha},\quad \mathrm{Le}=\frac{\upsilon}{D_B},\quad \rho=\sqrt{\frac{\upsilon}{aR^2}},\quad M=\frac{\beta_0^2\sigma}{a\rho},\quad Nb=\frac{\tau D_B}{\upsilon}\left(C_w-C\infty\right)$$
$$Nt=\frac{\tau D_t}{\upsilon T\infty}\left(T_w-T\infty\right),\quad \delta=\frac{Q_0}{a\rho Cp},\quad \gamma_1=\frac{h}{k}\sqrt{\tfrac{\upsilon}{a}},\quad \gamma_2=\frac{k_m}{D_m}\sqrt{\tfrac{\upsilon}{a}}\quad \text{and}\quad \tau=\frac{\left(\rho Cp\right)_p}{\left(\rho Cp\right)_f}$$

Here Pr, Le, ρ, M, Nb, Nt, δ, γ_1, and γ_2 donte the Prandtl number, the Lewis number, curvature parameter, magnetic field parameter, the Brownian motion parameter, the thermophoresis parameter, the heat source parameter, thermal Boit number, and concentration Boit number, respectively.

The OHAM procedure

In this section, the optimal homotopy asymptotic method (OHAM) used to solve the system eqs. (8)-(10) with the boundary conditions (11) under the following assumptions:

$$\mathcal{A}[f(\eta)]\equiv\mathcal{L}_f[f(\eta)]+\mathcal{N}_f[(\eta)] \tag{12}$$

$$\mathcal{B}[\theta(\eta),\phi(\eta),f(\eta)]\equiv\mathcal{L}_\theta[\theta(\eta)]+\mathcal{N}_f[\theta(\eta),\phi(\eta),f(\eta)] \tag{13}$$

$$\mathcal{C}[\phi(\eta),\theta(\eta),f(\eta)]\equiv\mathcal{L}_\phi[\phi(\eta)]+\mathcal{N}_f[\phi(\eta),\theta(\eta),f(\eta)] \tag{14}$$

Such that $\mathcal{L}_f[f(\eta)]$, $\mathcal{L}_\theta[\theta(\eta)]$, $\mathcal{L}_\phi[\phi(\eta)]$ are the linear operators of the system and takes the following forms:

$$\mathcal{L}_f[f(\eta)]=f'''(\eta)+k\,f''(\eta) \tag{15}$$

$$\mathcal{L}_\theta[\theta(\eta)]=\theta''(\eta)+k\,\theta'(\eta) \tag{16}$$

$$\mathcal{L}_\phi[\phi(\eta)]=\phi''(\eta)+k\,\phi'(\eta) \tag{17}$$

And $\mathcal{N}_f[f(\eta)]$, $\mathcal{N}_f[\theta(\eta),\phi(\eta),f(\eta)]$, $\mathcal{N}_f[\phi(\eta),\theta(\eta),f(\eta)]$ are the non-linear operators of the system, k is an unkown constant to be obtained to control the asymptotic behaviour of the solution.

Let the general solution of the system eqs. (8)-(10) to be:

$$f(\eta)=f_0(\eta)+\sum_{i=1}^{\infty}f_i(\eta) \tag{18}$$

$$\theta(\eta)=\theta_0(\eta)+\sum_{i=1}^{\infty}\theta_i(\eta) \tag{19}$$

$$\phi(\eta)=\phi_0(\eta)+\sum_{i=1}^{\infty}\phi_i(\eta) \tag{20}$$

Such that the initial guesses taken in the following form:

$$f_0(\eta)=\frac{1-e^{-k\eta}}{k},\quad \theta_0(\eta)=\left(\frac{1+\gamma_1}{\gamma_1}\right)e^{-k\eta}\quad\text{and}\quad \phi_0(\eta)=\left(\frac{1+\gamma_2}{\gamma_2}\right)e^{-k\eta} \tag{21}$$

The optimal homotopy equations defined:

$$(1-p)\ \mathcal{L}_f[F(\eta;p,a_n)]=p\,\mathcal{H}_f(\eta,a_n)\mathcal{A}[F(\eta;p,a_n)] \tag{22}$$

$$(1-p)\ \mathcal{L}_\theta[\Theta(\eta;p,b_n)]=p\,\mathcal{H}_\theta(\eta,b_n)\mathcal{B}[\Theta(\eta;p,b_n),\Phi(\eta;p,c_n),F(\eta;p,b_n)] \tag{23}$$

$$(1-p)\ \mathcal{L}_\phi[\Phi(\eta;p,c_n)]=p\,\mathcal{H}_\Phi(\eta,c_n)\mathcal{C}[\Phi(\eta;p,c_n),\Theta(\eta;p,b_n),F(\eta;p,b_n)] \tag{24}$$

where $p\in[0,1]$ denotes an embedding parameter and varies from 0 to 1 and $\mathcal{H}_f(\eta,a_n)$, $\mathcal{H}_\theta(\eta,b_n)$, and $\mathcal{H}_\Phi(\eta,c_n)$ are arbitary auxiliary convergence control functions.

Collecting the same powers of p, and equating each coefficient of p with zero, one can obtain the homotopy family equations. It is worth mentioning that, the solutions of the zero order equations p^0 are the initial guesses (21) which satisfied the boundary conditions (11).

The convergence of the solution depends on the choice of $\mathcal{H}_f(\eta,a_n),\mathcal{H}_\theta(\eta,b_n)$, and $\mathcal{H}_\Phi(\eta,c_n)$ whose assumed in the following form:

$$\mathcal{H}_f(\eta,a_n)=a_1\eta+(a_2+a_3\eta+a_4\eta^2+a_5\mathrm{e}^{-k\eta})\mathrm{e}^{-k\eta} \tag{25}$$

$$\mathcal{H}_\theta(\eta,b_n)=b_1+b_2\eta+(b_3+b_4\eta+b_5\eta^2+b_6\mathrm{e}^{-k\eta})\mathrm{e}^{-k\eta} \tag{26}$$

$$\mathcal{H}_\Phi(\eta,c_n)=c_1+c_2\eta+(c_3+c_4\eta+c_5\eta^2+c_6\mathrm{e}^{-k\eta})\mathrm{e}^{-k\eta} \tag{27}$$

To get the solution of the system, there are auxiliary constants k, a_n, b_n, c_n still undetermined, so the Galerkin method is applied to minimization the three residuals obtained $\mathcal{R}_f(\eta,a_n),\mathcal{R}_\theta(\eta,b_n)$, $\mathcal{R}_\Phi(\eta,c_n)$ as follows:

$$\int_0^\infty \mathcal{R}_f(\eta,a_n)\ell_i(\eta)\mathrm{d}\eta=0 \tag{28}$$

$$\int_0^\infty \mathcal{R}_\theta(\eta,b_n)\ell_i(\eta)\mathrm{d}\eta=0 \tag{29}$$

$$\int_0^\infty \mathcal{R}_\Phi(\eta,c_n)\ell_i(\eta)\mathrm{d}\eta=0 \tag{30}$$

where $\ell_i(\eta)$, $i=1:6$ are chosen functions taken:

$$\ell_1=1,\ \ell_2=\mathrm{e}^{-k\eta},\ \ell_3=\eta\,\mathrm{e}^{-k\eta},\ \ell_4=\eta^2\mathrm{e}^{-k\eta},\ \ell_5=\mathrm{e}^{-2k\eta},\ \ell_6=\eta\mathrm{e}^{-2k\eta} \tag{31}$$

For example, the general solution of the momentum eq. (8) at $\rho=0.5$, $M=0.5$ is:

$$f(\eta)=1.05677+\mathrm{e}^{-1.71872\eta}(9.10436-11.3328\mathrm{e}^{-3.43744\eta}+1.17169\mathrm{e}^{-1.71872\eta})+$$
$$+\eta\,\mathrm{e}^{-1.87955\eta}(-2.20775-16.0475\mathrm{e}^{-3.43744\eta}+1.98866\mathrm{e}^{-1.71872\eta})+$$
$$+\eta^2\mathrm{e}^{-1.71872\eta}(-10.1921-1.28195\mathrm{e}^{-3.43744\eta})+\eta^3\mathrm{e}^{-1.71872\eta}(-0.381924-7.12911\mathrm{e}^{-3.43744\eta})$$

Such that: k =1.71872, $a_1=63.0291$, $a_2=-96.6372$, $a_3=49.0117$, $a_4=\ =-61.523$, $a_5=-1.14577$.

To check the accuracy of the obtained results, a compression between the present results and the results of Hayat *et al.* [14] shown in tab. (1)

Table 1. Compression between the present results and previous published results for $f''(0)$

	$\rho = 0, M = 0$	$\rho = 0, M = 0.4$	$\rho = 0, M = 10$
Present results OHAM	–1.0048	–1.45932	–3.3166
Previous results	–1.0042 [22]	–1.45934 [14]	–3.3165 [22]

Physical aspect

Physically, the problem deals to investigate the skin friction coefficient, and Nusselt/ Sherwood numbers whose indicate to surface shear stress and rate of heat and mass transfer respectively.

Surface shear stress:

$$\tau_w = \mu\left(\frac{\partial u}{\partial y}\right)_{r=R} = \mu\, U_w\sqrt{\frac{a}{\upsilon}} f''(0) \tag{32}$$

since the skin friction coefficient is given by:

$$C_f = \frac{2\tau_w}{\rho U_w^2} \quad i.\,e. \quad 2f''(0) = \sqrt{\mathrm{Re}}\, C_f \tag{33}$$

Surface heat flux:

$$q_w = -k\left(\frac{\partial T}{\partial r}\right)_{r=R} = -k\,\left(T_f - T_\infty\right)\sqrt{\frac{a}{\upsilon}}\theta'(0) \tag{34}$$

since the Nusselt number is given:

$$\mathrm{Nu} = \frac{x\, q_w}{k(T_f - T_\infty)} \quad i.\,e. \quad \frac{\mathrm{Nu}}{\sqrt{\mathrm{Re}}} = -\theta'(0) \tag{35}$$

Surface mass flux:

$$q_m = -D_B\left(\frac{\partial C}{\partial r}\right)_{r=R} = -D_B(C_f - C_\infty)\sqrt{\frac{a}{\upsilon}}\ \varphi'(0) \tag{36}$$

since the Sherwood number is given:

$$\mathrm{Sh} = \frac{x\, q_m}{D_B(C_f - C_\infty)} \quad i.\,e. \quad \frac{\mathrm{Sh}}{\sqrt{\mathrm{Re}}} = -\varphi'(0) \tag{37}$$

Discussions

The present work provides a mathematical model to the process of cooling of a moving cylinder in a nanofluid and subjected to bottom hot fluid and normal magnetic field as well as heat source. The influence of all embedded parameters on the velocity, temperature and nanoparticles concentration within the boundary-layer are shown in figs. 2-14. The Prandlt number of the base fluid (water) is kept constant at 7. Moreover, tabs. 2-5 show the effect of all embedded parameters on the surface skin friction, Nusselt number and Sherwood number.

The curvature parameter is the parameter which controls the surfaces shape such that for $\rho = 0$ the problem transformed to flat surface. The effect of this parameter on the velocity, temperature, and nanoparticle concentration appears through figs. 2-4. One can observe that the increasing of surface curvature increases the velocity, temperature, and nanoparticle concentration. Also fig, 3 depict that the temperature at the surface has no change with the increasing or decreasing of curvature parameter. On the other hand, the effect of curvature parameter on the surface skin friction, surface heat flux, and surface mass flux presented in tab. 2. One can observe that the surface skin friction, heat flux, and mass flux are higher in the case of cylinder than the case of flat surface.

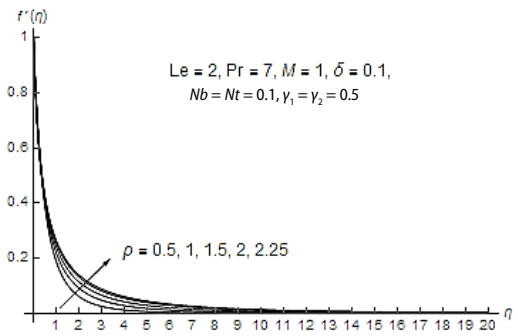

Figure 2. The velocity profiles with increasing of curvature parameter ρ

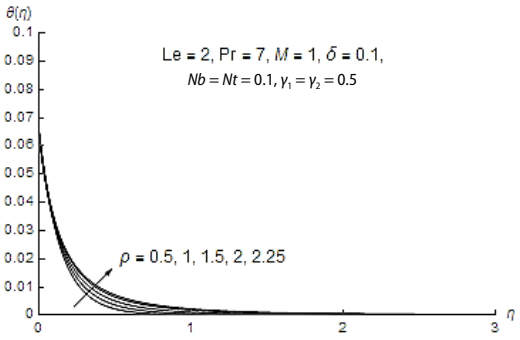

Figure 3. The temperature profiles with increasing of curvature parameter ρ

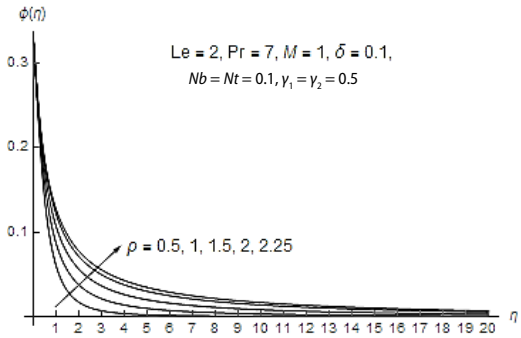

Figure 4. The concentration profiles with increasing of curvature parameter ρ

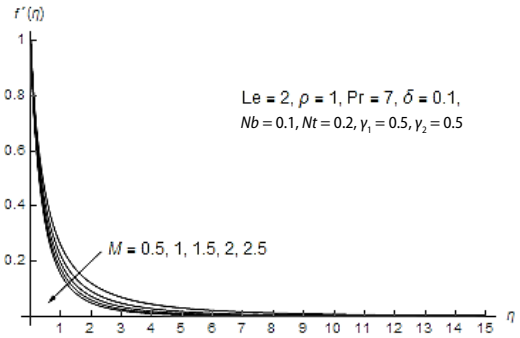

Figure 5. The velocity profiles with increasing of magnetic field parameter M

The effect of magnetic field on the velocity and nanoparticles concentration showed in figs. 5 and 6. One can observe that the increasing of the magnetic parameter decreases the velocity, temperature, and increase nanoparticle concentration.

On the other hand, tabs. 2 and 3 confirm that using MHD flow as a cooling medium increases the skin friction and decrease Nusselt number as well as the Sherwood number by limited values. Consequently, the surface shear stress increases and rate of heat transfer and rate of mass transfer decrease by increasing of magnetic parameter, M.

The effect of thermal and concentration boit numbers on the temperature and nanoparticles concentration showed in figs. 7-9. It is clear that the temperature and nanoparticle concentration both increase by increasing of thermal boit number and concentration Boit number.

Table 2. Values of velocity gradient, temperature gradient, and concentration gradient at the surface at $Nt = Nb = \delta = 0.1$, $M = 1$, Pr = 7, $\gamma_2 = 0.5$

ρ	γ_1	$\frac{1}{2}\sqrt{\mathrm{Re}}C_f$	$\mathrm{Nu}/\sqrt{\mathrm{Re}}$	$\mathrm{Sh}/\sqrt{\mathrm{Re}}$
0	0.10	–2.000000	–0.109886	–0.699383
	0.20	–2.000000	–0.238933	–0.691576
	0.30	–2.000000	–0.386422	–0.683984
2	0.10	–2.711306	–0.109868	–0.702305
	0.20	–2.711306	–0.238954	–0.693641
	0.30	–2.711306	–0.386491	–0.685191

Moreover, the effect of these parameters on the surface skin friction, Nusselt number, and Sherwood number presented in tabs. 2 and 3. By investigation, one can observe that Nusselt number increases by increase of thermal and concentration Boit numbers but the Sherwood number increases by concentration boit numbers and opposite effect appears with thermal Boit number which consequently affected on the rate of heat and mass transfer.

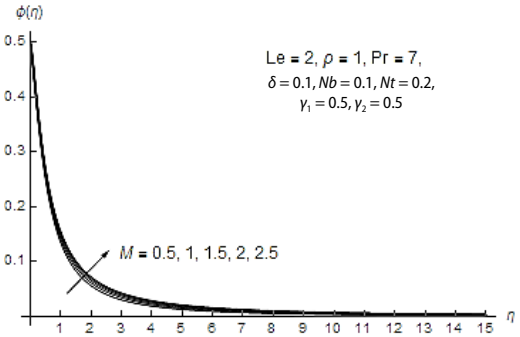

Figure 6. The concentration profiles with increasing of magnetic field parameter M

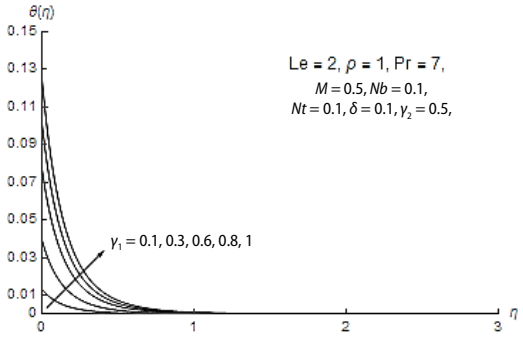

Figure 7. The temperature profiles with increasing of thermal Boit number γ_1

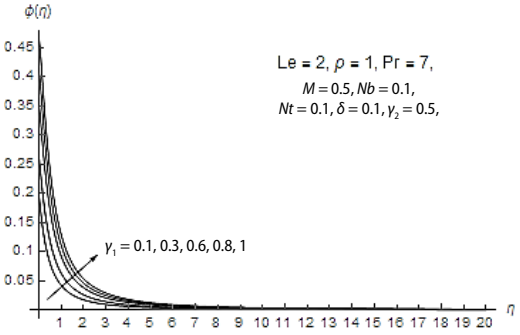

Figure 8. The concentration profiles with increasing of thermal Boit number γ_1

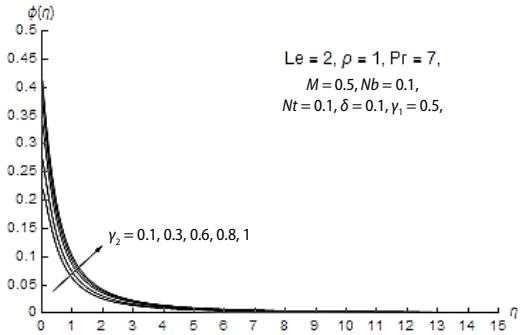

Figure 9. The concentration profiles with increasing of concentration Boit number γ_2

Brownian motion is the random moving of particles suspended in a fluid (nanoparticles) resulting from their bombardment by the fast-moving atoms or molecules in the fluid. This motion controls the temperature and the concentration of the particles within the boundary-layer over the surface. The Brownian motion parameter, *Nb,* is the key of this mechanism such that the increasing of *Nb* leads to increasing of the boundary-layer temperature and decreasing of the nanoparticles concentration as shown in figs. 10 and 11. On the other hand, the effect of Brownian motion on the temperature gradient, concentration gradient and the corresponding values of Nusselt number, Sherwood number presented in tab. 4. It is clear that this motion decreases the rate of heat and mass transfer by decreasing the Nusselt number, Sherwood number.

Thermophoresis is a phenomenon observed in mixtures of mobile particles where the different particle types exhibit different responses to the force of a temperature gradient. Explain this phenomenon appears in this study through the thermophoresis parameter, *Nt,* such that increasing this parameter leads to increasing of boundary-layer temperature and nanoparticles concentration as shown in figs. 12 and 13.

Table 3. Values of velocity gradient, temperature gradient, and concentration gradient at the surface at $Nt = Nb = \delta = 0.1$, $M = 0.5$, $\mathrm{Pr} = 7$, $\gamma_1 = 0.5$

ρ	γ_2	$\frac{1}{2}\sqrt{\mathrm{Re}}C_f$	$\mathrm{Nu}/\sqrt{\mathrm{Re}}$	$\mathrm{Sh}/\sqrt{\mathrm{Re}}$
1	0.00	–2.368738	–0.734086	–0.107750
	1.00	–2.368738	–0.734011	–0.229878
	2.00	–2.368738	–0.733940	–0.364874
2	0.00	–2.711306	–0.734233	–0.107717
	1.00	–2.711306	–0.734159	–0.229810
	2.00	–2.711306	–0.734090	–0.364846

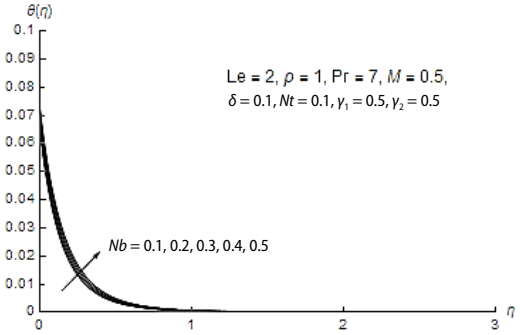

Figure 10. The temperature profiles with increasing of Brownian motion parameter *Nb*

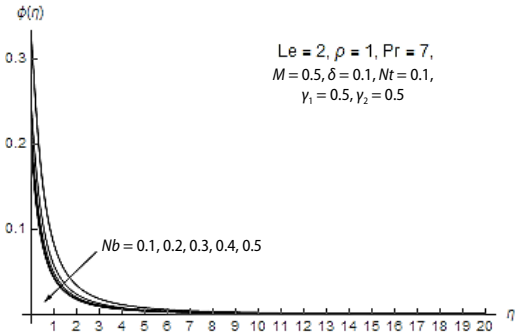

Figure 11. The concentration profiles with increasing of Brownian motion parameter *Nb*

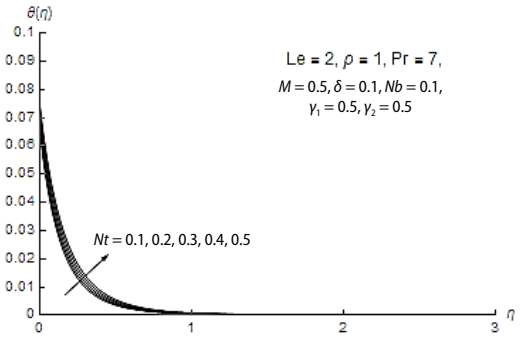

Figure 12. The temperature profiles with increasing of the thermophoresis parameter *Nt*

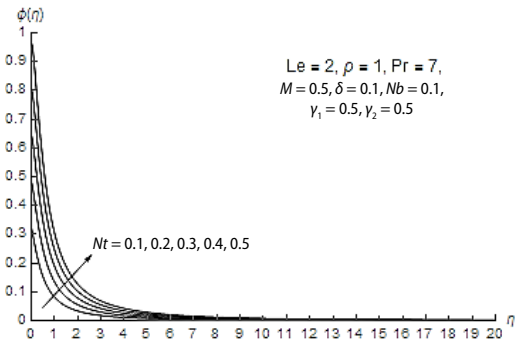

Figure 13. The concentration profiles with increasing of the thermophoresis parameter *Nt*

It is worth mentioning that the thermophoresis parameter is possible to be a positive or negative signal such that the negative value of *Nt* indicates to hot surface while positive to cold surface. Moreover, for hot surfaces, thermophoresis tends to blow the nanoparticles concentration boundary-layer away from the surface since a hot surface repels the sub-micron sized particles from it, thereby forming a relatively particle free layer near the surface.

On the other hand, the effect of thermophoresis parameter on the temperature gradient, concentration gradient and the corresponding values of Nusselt number, Sherwood number

shown in tab. 4. it is clear that the increasing of thermophoresis parameter decreases the rate of heat transfer and increase mass transfer.

The effect of heat source parameter, δ, on the temperature is shown in fig. 14. As expected, the increasing of δ leads to increasing of boundary-layer. Moreover, tab. 5 shows the effect of this parameter on the temperature gradient and the corresponding values of Nusselt number. The results obtained in this table indicate that the increasing of heat source parameter leads to decreasing of Nusselt number and heat transfer from the surface.

Table 4. Values temperature gradient and concentration gradient at the surface at $\rho = 1$, $M = 0.5$, $\delta = 0.1$, Pr = 7, and Le = 2

Nt	$\mathrm{Nu}/\sqrt{\mathrm{Re}}$	$\mathrm{Sh}/\sqrt{\mathrm{Re}}$
0.1	–0.733847	–0.669420
0.2	–0.733316	–0.629311
0.3	–0.732752	–0.589217
Nb	$\mathrm{Nu}/\sqrt{\mathrm{Re}}$	$\mathrm{Sh}/\sqrt{\mathrm{Re}}$
0.1	–0.733847	–0.669420
0.2	–0.733391	–0.689485
0.3	–0.732913	–0.696174

Table 5. Values of temperature gradient and concentration gradient at the surface at $Nt = Nb = 0.1$, $M = 0.5$, Pr = 7, $\rho = 1$, $\gamma_1 = \gamma_2 = 0.5$

δ	$\mathrm{Nu}/\sqrt{\mathrm{Re}}$	$\mathrm{Sh}/\sqrt{\mathrm{Re}}$
–1.00	–0.147133	–0.669395
–0.50	–0.146990	–0.669405
0.00	–0.146811	–0.669417
0.50	–0.146572	–0.669431
1.00	–0.146183	–0.669449

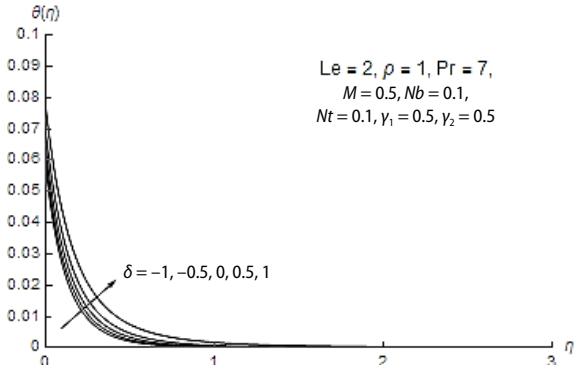

Figure 14. The temperature profiles with increasing of the heat source parameter δ

Conclusion

This study provides a mathematical model of a continuous moving cylinder embedded into a MHD nanofluid under the effect of convective boundary conditions, Brownian motion, thermophoresis force. The following results are obtained:

- Boundary-layer velocity increases in the presence of curvature parameter and the absence of magnetic parameter.
- Boundary-layer temperature increases in the presence curvature parameter, thermal Boit parameter, thermophoresis parameter, Brownian motion parameter, and heat source parameter
- Nanoparticles concentration increases with increase of magnetic parameter, thermal and concentration Boit parameters, and thermophoresis parameter and the opposite is true with Brownian motion parameter.
- The rate of heat and mass transfer over the surface increase in the presence of thermal and concentration Boit parameters by increasing the values of Nusselt and Sherwood number.

- Generally, the rate of heat and mass transfer over the cylindrical surface is large than that in the case of flat surface [4], but this study indicates that this increase may be reduced in the presence of convictive boundary conditions.

References

[1] Chamkha, A., Heat and Mass from MHD Flow over a Moving Permeable Cylinder with Heat Generation or Absorption and Chemical Reaction, *Communications in Numerical Analysis*, *1* (2011), 1, pp.1-19
[2] Swati, M., Analysis of Boundary Layer Flow and Heat Transfer Along a Stretching Cylinder in a Porous Medium, *Thermodynamics*, *1* (2012), 1, pp.1-7
[3] Elbashbeshy, E. M. A., *et al*., Effects of Magnetic Field on Flow and Hear Transfer Over a Stretching Horizontal Cylinder in The Presence of a Heat Source/Sink with Suction/Injection, *Applied Mechanical Engineering*, *1* (2012), 1, pp.1-5
[4] Rekha, R., Naseem, A., Boundary Layer Flow Past a Stretching Cylinder and Heat Transfer with Variable Thermal Conductivity, *Applied Mathematics*, *3* (2012), 1, pp. 205-209
[5] Choi, S. U. S., Enhancing Conductivity of Fluids with Nanoparticles, *ASME International Mechanical Engineering Congress & Exposition*, *231* (1995), 1, pp. 99-105
[6] Azizah, M., *et al*., Flow and Heat Transfer over an Unsteady Shrinking Sheet with Suction in Nanofluids, *Int. J. Heat and Mass Transfer*, *55* (2011), 7, pp. 1888-1897
[7] Aminreza, N., *et al*., Effect of Partial Slip Boundary Condition on The Flow and Heat Transfer of Nanofluids Past Stretching Sheet Prescribed Constant Wall Temperature, *Int. J. of thermal Sci*., *54* (2012), 1, pp. 253-261
[8] Hamad, M., Analytical Solution of Natural Convection Flow of Nanofluids over a Linearly Stretching Sheet in The Presence of Magnetic Field, *International Communications in Heat and Mass Transfer, 38* (2011), 4, pp. 487-492
[9] Alsaedi, A., *et al*., Effects of Heat Generation/Absorption on Stagnation Point Flow of Nanofluid over a Surface with Convective Boundary Conditions, *Communication in Nonlinear & Sci. Numerical Simulation*, *17* (2012), 11, pp. 4210-4223
[10] Elbashbeshy, E. M. A., *et al*., An Exact Solution of Boundary Layer Flow over a Moving Surface Embedded into a Nanofluid in the Presence of Magnetic Field and Suction/Injection, *Heat Mass Transfer*, *50* (2014), 1, pp. 57-64
[11] Elbashbeshy, E. M. A., *et al*., Flow and Heat Transfer over a Moving Surface with Non-Linear Velocity and Variable Thickness in a Nanofluid in the Presence of Thermal Radiation, *Can. J. Phys*., *92* (2013), 2, pp. 124-130
[12] Abdel-Wahed, M. S., *et al*., Flow and Heat Transfer over a Moving Surface with Non-Linear Velocity and Variable Thickness in a Nanofluid in the Presence of Brownian Motion, *Applied Mathematics and Computation*, *254* (2015), 1, pp. 49-62
[13] Abdel-Wahed, M. S., Flow and Heat Transfer of a Weak Concentration Micropolar Nanofluid over Steady/Unsteady-Moving Surface, *Appl. Phys. A*., *123* (2017). 195, pp. 1-10
[14] Hayat, T., *et al*., MHD Flow of Nanofluid over Permeable Stretching Sheet with Convective Boundary Conditions, *Thermal Science*, *20* (2016), 6, pp. 1835-1845
[15] Nazar, R., *et al*., Mixed Convection Boundary Layer Flow from a Horizontal Circular Cylinder Embedded in A Porous Medium Filled with A Nanofluid, *Transp. Porous Med.*, *86* (2011), 1, pp. 517-536
[16] Anbuchezhian, N., *et al*., Thermophoresis and Brownian Motion Effects on Boundary Layer Flow of Nanofluid in Presence of Thermal Stratification Due to Solar Energy, *Applied Mathematics & Mechanics, 33* (2012), 6, pp. 765-780
[17] Ali, J., *et al*., Transient Natural Convection Flow of a Nanofluid over a Vertical Cylinder, *Meccanica*, *48* (2013), pp. 71-81
[18] Elbashbeshy, E. M. A., *et al*., Effect of Heat Treatment Process with a New Cooling Medium (Nanofluid) on the Mechanical Properties of an Unsteady Continuous Moving Cylinder, *Journal of Mechanical Science and Technology*, *27* (2013),12, pp. 3843-3850
[19] Elbashbeshy, E. M. A., *et al*., The Effect of Thermal Radiation and Heat Generation on the Mechanical Properties of Unsteady Continuous Moving Cylinder in a Nanofluid in the Presence of Suction or Injection, *American Journal of Mechanical Engineering and Automation*, *1* (2015), 3, pp. 24-30
[20] Abdel-Wahed, M. S., Akl, M., Effect of Hall Current on Mhd Flow of a Nanofluid with Variable Properties Due to a Rotating Disk with Viscous Dissipation and Nonlinear Thermal Radiation, *AIP Advances, 6* (2016), 9, 095308

[21] Abdel-Wwahed, M. S. Emam, T. G., Effect of Joule Heating and Hall Current on Mhd Flow of a Nanofluid Due to a Rotating Disk with Viscous Dissipation. *Thermal Sciences*, *22* (2016), 2, pp. 857-870
[22] Nadeem, S., *et al*., Mhd Three-Dimensional Boundary Layer Flow of Casson Nanofluid Past a Linearly Stretching Sheet with Convective Boundary Condition, *IEEE Transactions on Nanotechnology*, *13* (2014), 1, pp. 109-115

Paper submitted: September 11, 2017
Paper revised: July 22, 2018
Paper accepted: September 6, 2018